Influence of zirconium concentration on optical characteristics of nanostructured zirconium diselenite inorganic cation exchanger

J. HENRY, K. MOHANRAJ*, S. KANNAN, S. BARATHAN[a], G. SIVAKUMAR[b]
Department of Physics, Manonmaniam Sundaranar University, Tirunelveli-627 012, Tamil Nadu, India
[a]*Department of Physics, Annamalai University, Annamalai Nagar-608 002, Tamil Nadu, India*
[b]*CISL, Department of Physics, Annamalai University, Annamalai Nagar-608 002, Tamil Nadu, India*

Zirconium diselenite ($Zr(SeO_3)_2$) nanoparticles have been synthesized using three different molar concentrations (0.25:1, 0.5:1 and 0.75:1) of $ZrO(NO_3)_2.xH_2O$ and SeO_2 by precipitation method. The synthesized particles have been characterised using XRD, FTIR, FESEM and UV-Visible spectroscopy. From the XRD result, the zirconium diselenite particles are orthorhombic structure and better crystallinity is noticed in 0.25:1M concentration compared to other two concentrations. The FTIR result is confirmed the presence of $Zr(SeO_3)_2$ in all the three spectrum at 885 cm^{-1}, 739 cm^{-1} and 491 cm^{-1} and from the FESEM images, cubic, hexagonal and polygonal shapes of $Zr(SeO_3)_2$ particles are detected. In the UV-Visible analysis, optical absorption is higher for 0.25: 1M concentration in the visible region when compared to other two concentrations and maximum optical absorption is found around 387 nm and band gap energy of the samples is found to be around 3.95eV.

Received December 3, 2012; accepted September 18, 2013)

Keywords: Zirconium diselenite, Precipitation method, XRD, FESEM, FTIR

1. Introduction

In the middle of the last century, an ion-exchange process was studied and the first commercially available ion-exchangers were amorphous aluminosilicate gel. This exchanger is known to be unstable towards the acidic solutions. Hence, it led chemists to find alternatives. The search eventually led to the synthesis of the first organic ion-exchange resins which dominated the field until the post world war II era. The advent of nuclear technology initiated a search for inorganic ion exchange materials that would remain stable above 150 °C and in high radiation fields.

The uses of inorganic ion-exchangers have been explored only in the beginning of the last two decades. Since then the analytical applications of synthetic inorganic ion-exchangers have attracted great attention. The important features of these materials are: the differential selectivity, the ease of preparation extra stability under ionizing radiations and at high temperature. It is inspired the authors to prepare the inorganic ion-exchange. To know to our knowledge, there is found a few literatures in the globe for preparation of zirconium diselenite using zirconium oxide as starting material [1, 2]. However, the authors are not reported the optical and structural properties of zirconium diselenite. Hence, objective of the study is to prepare the zirconium diselenite nanoparticles using zirconyl nitrate as a starting material and study the structural and optical properties.

2. Experimental procedure

To synthesize zirconium diselenite nanoparticles, A.R Grade of $ZrO(NO_3)_2.xH_2O$ and SeO_2 were taken in three different molar ratio 0.25:1, 0.5:1 & 0.75:1. The both solutions were stirred individually in double distilled water until dissolved well. Then the solutions were mixed together and again stirred vigorously about 5 hours at room temperature. A white precipitate was obtained which was thoroughly washed using ethanol and water, and then dried in an oven at 60 °C for two hours. The powder samples were grained by using agate mortar and pestle.

Crystalline phases of the $Zr(SeO_3)_2$ nanoparticles were investigated by PANalytical X'PERT PRO diffractometer with Cu Kα monochromatic radiation source (λ=1.5406 Å) in the range of 2θ=10˚- 80˚. Molecular vibrations of the $Zr(SeO_3)_2$ nanoparticles were carried out using Perkin Elmer FTIR spectrometer (Model RX-I) with the wavelength range of 4000 – 400 cm^{-1}. FESEM images were taken by FESEM curl-Zeiss instrument. Optical transmission and absorbance characterization of the particles were recorded using JASCO UVIDEC – 650 UV-Vis Spectrophotometer in the range 300 to 800 nm.

3. Result and discussion

The XRD patterns of $Zr(SeO_3)_2$ nanoparticles are shown in Fig.1(a-c). In the XRD pattern (Fig.1 (a)), some strong intensity peaks at 2θ= 21.73˚, 24.95˚, 27.55˚ and 28.36˚ which are owing to the planes of (2 0 1), (2 1 0), (2 1 2) and (0 2 1) reflections respectively of

orthorhombic crystal structure (JCPDS no. 50-0336) with lattice parameters a=8.5549 Å, b=6.479 Å and c=15.2317 Å.

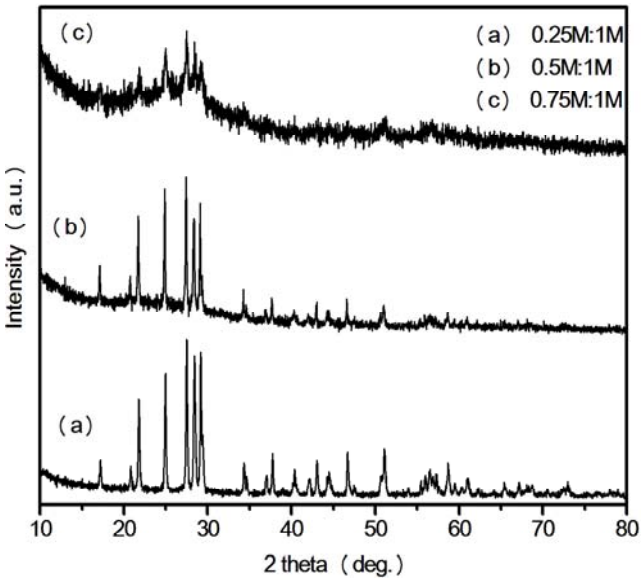

Fig. 1. XRD patterns of $Zr(SeO_3)_2$ nanoparticles prepared at different molar ratios .

In addition, a peak at 2θ=29.1˚ which belongs to the plane of (1 0 0) reflection of hexagonal structure (JCPDS. no. 15-0249) of Zr_3Se_2 as impurity. In the XRD pattern of 0.5:1M, intensity of the crystalline peaks get reduced and it is more in 0.75:1M. The result may be due to increase the concentration of zirconium leads to form zirconium selenite ($ZrSeO_3$) which prevents the formation of $Zr(SeO_3)_2$. However, zirconium selenite peaks are not shown in the XRD patterns. This result is in agreement with the early report by V. P. Nesterenko [2]. According to the author, selenious acid should be taken as 10 time excess than zirconium solution to prevent the formation of zirconium selenite. The following equation [3, 4] can be explained the formation of $Zr(SeO_3)_2$ nanoparticles:

$$ZrO(NO_3)_2.xH_2O \rightarrow ZrO^{2+} + 2(NO_3)^- + xH_2O \quad (1)$$

$$H_2SeO_3 \rightarrow 2H^+ + (SeO_3)^{2-} \quad (2)$$

$$ZrO^{2+} + H_2SeO_3 \rightarrow ZrOSeO_3 + 2H^+ \quad (3)$$

$$ZrOSeO_3 + H_2SeO_3 \rightarrow Zr(SeO_3)_2 + H_2O \quad (4)$$

The peak broadening in the XRD pattern at lower angle is more meaningful for calculation of grain size. The average grain sizes of all the zirconium diselenite samples were calculated using the Scherrer's formula. $D=k\lambda/\beta\cos\theta$, where D is the crystalline size, k is the Scherrer's constant (k=0.9), λ the wavelength of the X-ray, β the full-peak width at half of the maximum intensity after correction for the instrument-broadening contributions and θ the peak position [5].

Dislocations are the imperfections in a crystal and associated with the mis-registry of the lattice in one part of the crystal with respect to another part. Unlike vacancies and interstitial atoms, dislocations are not equilibrium imperfections. In fact, the growth mechanism involving dislocations is a matter of importance. The dislocation densities are given by the Williamson and smallman's relation. $\delta=n/D^2$, where δ is dislocation density, n is a factor, which equals unity, giving minimum dislocation density and D is the grain size [6].Table 1 gives value of the grain size and dislocation density of all prepared samples.

Fig. 2 show the FTIR spectra of $Zr(SeO_3)_2$. In Fig. 2. (a), a medium intensity band is observed at 1650 cm^{-1} which is due to hydroxyl groups of molecular water [7] and a strong band is noticed around 739 cm^{-1} which may be due to either the asymmetric stretching vibration of Zr-O_2-Zr or the stretching of Se-O bonds in the SeO_3^{2-} anions [8, 9]. According to the author, H. R. Sahu et al., [8] have assigned the band at 739 cm^{-1} which is due to asymmetric stretching vibration of Zr-O_2-Zr while

Table 1. Grain size of $Zr(SeO_3)_2$ nanoparticles at different conditions

S.No.	Molar ratio	Grain size (nm)	Dislocation density (10^{14} lin/m^2)
1	0.25:1	78.06	1.6
2	0.5:1	42.13	5.6
3	0.75:1	27.17	13

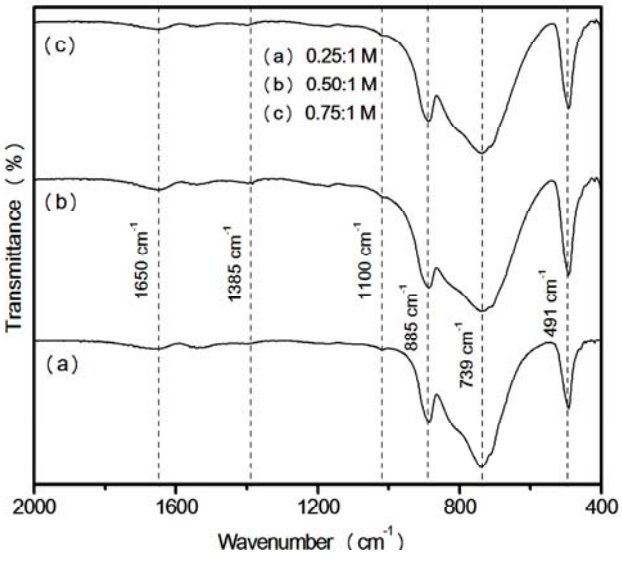

Fig. 2. FTIR spectra of $Zr(SeO_3)_2$ nanoparticles prepared at different molar ratios

J. Ling et al., [9] have assigned the same band due to Se-O bond. Also, a strong band appears in the spectrum at 491 cm^{-1} which is due to the stretching vibration of Zr-O [8, 10] and it is confirmed the presence of Zr ions. A band shown at 885 cm^{-1} which is due to stretching vibrations of Se-O bonds [9] and a hump is noticed at 1100 cm^{-1} which is owing to the Zirconia [8]. The peak which appears at

1385 cm^{-1} is due to the bending vibration of Zr–OH group [11].

In Fig. 2. (b & c) the characteristic $Zr(SeO_3)_2$ bands are observed at 1385, 1100, 885, 739 and 491 cm^{-1} which are similar position as that of 0.25:1 M of $Zr(SeO_3)_2$ (Fig. 2. (a)).

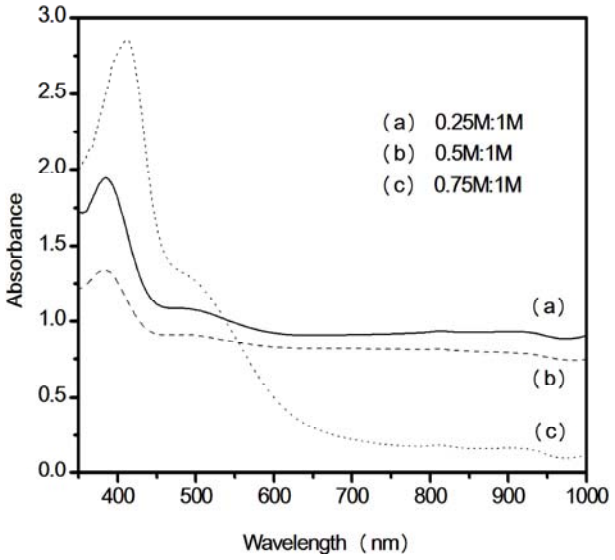

Fig. 3: UV-VIS absorption spectra of $Zr(SeO_3)_2$ nanoparticles prepared at different molar ratios

Fig.3. shows the UV-Visible spectra of zirconium diselenite particles prepared in different molarities. In the three spectrum, maximum optical absorption is found around 385 nm and starts to decrease around 400 nm and became a linear variation is observed in the visible region. However, maximum absorption of 0.75:1 M of $Zr(SeO_3)_2$ starts to decrease from 500 nm. It can be regarded as an excitonic peak for $Zr(SeO_3)_2$ nanoparticles and proves the existence of $Zr(SeO_3)_2$ nanoparticle. The results are in agreement with the earlier reports of $(SeO_3)_2$ composite materials [9]. The peaks in the absorption spectrum shift to lower wavelength from 413 to 385nm which is due to the increase in particle size from 0.75M to 0.25M. It implies that the optical properties are strongly dependent on the particle size [12].

To determine the optical band gap, the following dependence of α on photon energy was used $(\alpha h\nu)\ \alpha\ (h\nu - E_g)^n$ where E_g is band gap; α is absorption coefficient; n is an index that can assume values of (1/2, 2), depending on the nature of electronic transitions. For the direct allowed transitions, n has a value of 1/2 while for indirect allowed transitions n=2. The optical band gaps for direct transitions are evaluated from the plot of $(\alpha h\nu)^2$ Vs $(h\nu)$ (Fig.4). The plot for direct transitions shows a straight line and yields a value in the range from 3.93 to 3.98 eV. The band gap results are comparable with the literature for the $(SeO_3)_2$ composite materials [13-14]. Light absorption leads to an electron in the conduction band and a positive hole in the valence band. In small particles they are confirmed to potential wells of small lateral dimension and the energy difference between the position of conduction band and a free electron, which leads to a quantization of their energy levels. The phenomena arise when the size of the particles becomes comparable to de Broglie wavelength of a charge carrier. The increase in the band gap of as-prepared $Zr(SeO_3)_2$ nanoparticles is an indication of size quantization effects [15]

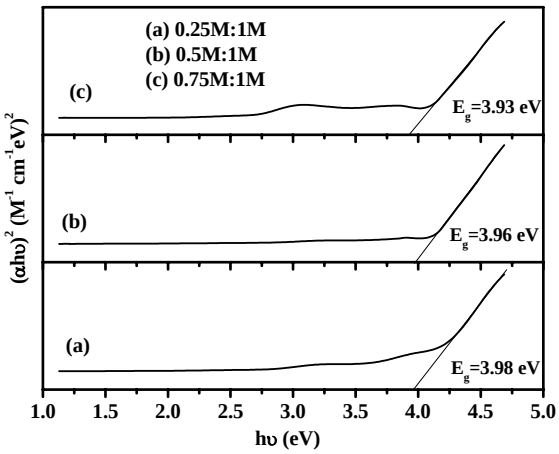

Fig.4: The plot of $(\alpha h\nu)^2$ Vs $(h\nu)$

The FESEM images of 0.5M: 1M of zirconium diselenite nanoparticle is shown in Fig. 5 (a & b). The $Zr(SeO_3)_2$ particles are found to be different shapes in the photograph like cubes, hexagons and polygonal (Fig. 5 (a)) which are dispersed on the surface and are more compact structure. The observed results are clearly seen in the higher magnification image (Fig. 5 (b)).

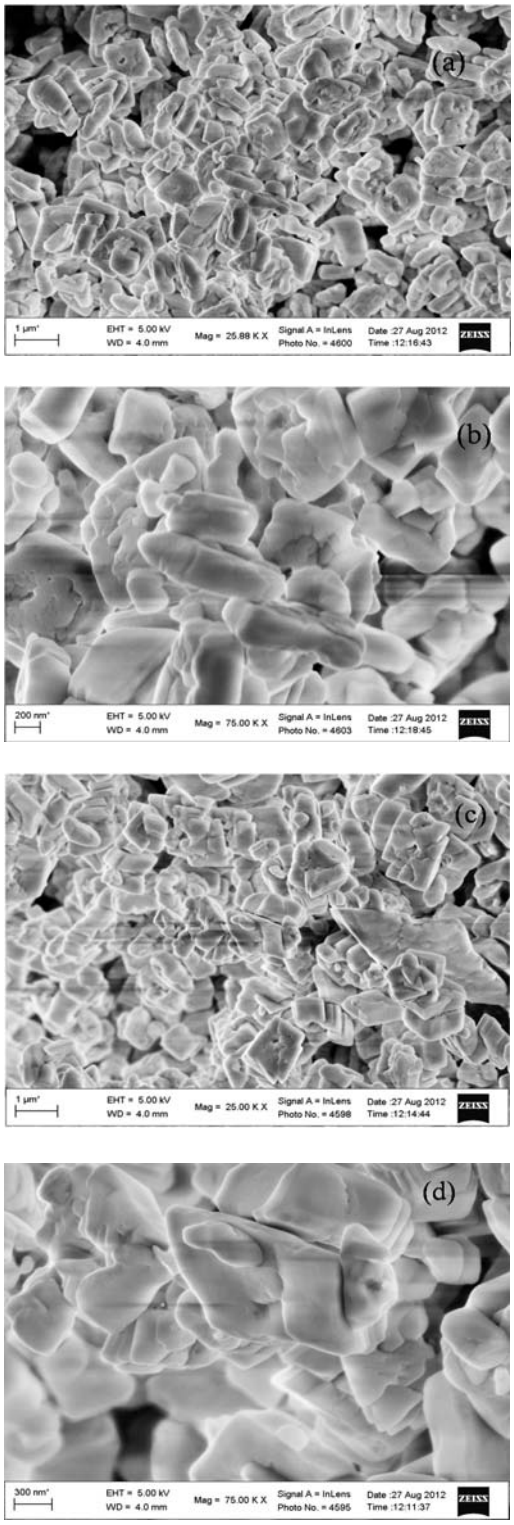

Fig. 5.FESEM image of 0.5:1M ((a) low and (b) high magnification) and 0.75:1M ((c) low and (d) high magnification) of ($Zr(SeO_3)_2$).

The FESEM images of 0.5M: 1M of zirconium diselenite nanoparticle is shown in Fig. 5 (a & b). The $Zr(SeO_3)_2$ particles are found to be different shapes in the photograph like cubes, hexagons and polygonal (Fig. 5 (a)) which are dispersed on the surface and are more compact structure. The observed results are clearly seen in the higher magnification image (Fig. 5 (b)).

The average particle size of zirconium diselenite is found to be 200 nm. The Fig. 5 (c & d) shows the FESEM image of 0.75M: 1M of zirconium diselenite particles. In the photograph, particle shapes are similar as that of 0.5:1 M of zirconium diselenite. The average size of the particles are found to be around 220 nm which is slightly bigger than 0.5:1 M of $Zr(SeO_3)_2$ It may be due to the increase of Zirconium in the mixture.

4. Conclusion

In this report, we have synthesized zirconium diselenite nanoparticles ($Zr(SeO_3)_2$) using three different molar concentration (0.25:1M, 0.5:1M and 0.75:1M) of $ZrO(NO_3)_2.xH_2O$ and SeO_2 by precipitation method. From the XRD results, zirconium diselenite particles are found to be orthorhombic crystal structure and the average grain size is found to be 78.06 for 0.25:1M, 42.13 for 0.5 M and 27.17 nm for 0.75:1 M. The FTIR results are confirmed the presence of zirconium diselenite in all the spectrum at 885 cm^{-1}, 739 cm^{-1} and 491 cm^{-1}. The FESEM images are evidenced for cubic, hexagonal and polygonal shape of the zirconium diselenite particles. From the optical absorption study, maximum absorption is found around 387 nm for all the three samples. However, the 0.75:1 M of zirconium diselenite has shift around 500 nm when compared to other two samples which are shift around 400 nm. The average band gap energy of the samples is found to be 3.95 eV. From the above experimental results, it is concluded that 0.25:1 M concentration of zirconium diselenite particles have better crystalline than other two concentrations.

Acknowledgement

The authors are thankful to the UGC-SAP, New Delhi for providing the financial support to the Department of Physics, Manonmaniam Sundaranar University, Tirunelveli, Tamil Nadu, India and the Prof. and Head, Department of Physics, Annamalai University for providing the analytical instrumentation facilities.Also the authors are thankful to the authorities of the Manonmaniam Sundaranar University, Tirunelveli for providing the seed money project to carry out the work.

References

[1] N. Retta, T. Sisly, Bull. Chem. Soc. Ethiop. **8**, 1 (1994).
[2] V. P. Nesterenko, J. Thermal analysis and calorimetry **80**, 575 (2005).
[3] A. M. Sargar, N. S .patil, S.R. Mane, S. N. Gawale, P. N. Bhosale, Int. J. Electrochem. Sci. **4**, 887 (2009).
[4] S. G. Simpson, W. C. Schums, Cambridge, Massachusetts 921 (1934).

[5] P. Manivasakan, V. Rajendran, P. R. Rauta, B. B. Sahu, B. K. Panda, J. Am. Ceram. Soc. **94**, 1410 (2011).
[6] Rahul, S. R. Vishwakarma, R. N. Tirupathi, A. K. Verma, The African review of physics **6**, 103 (2011).
[7] C. Y. Tai, B. Hsiao, H. Chiu, Colloids and surfaces A: Physicochem.E ng. Aspects **237**, 105 (2004).
[8] H. R. Sahu, G. R. Rao, Bull. Mater. Sci. **23**, 349 (2000).
[9] J. Ling, T. E. Albrecht-Schmitt, J. Solid state chem. **180**, 1607 (2007).
[10] K. Geethalakshmi, T. Prabhakaran, J. Hemalatha, World Academy of Science, Engineering and Technol. **64,** 179 (2012).
[11] D. Sarkar, D. Mohapatra, S. Raya, S. Bhattacharyya, S. Adaka, N. Mitra, Ceramics International **33**, 1275 (2007).
[12] P**.** Gupta**,** M. Ramrakhiani**,** The Open Nanoscience Journal **3,** 15 **(**2009**).**
[13] S. Zhang, C. Hu, P. Li, H. Jiang, J. Mao, Dalton Trans.**41**, 9532 (2012).
[14] F. Kong, C. Hu, X. Xu, T. Zhou, J. Mao, Dalton Trans. **41**, 5687 (2012).
[15] Y. Zhao, X. H. Liao, J. M. Hong, J. J. Zhu, Mater. Chem. Phys. **87**, 149 (2004).

*Corresponding author: kmohanraj.msu@gmail.com